European Journal of Pharmaceutics and Biopharmaceutics 115 (2017) 52–64

Contents lists available at ScienceDirect

European Journal of Pharmaceutics and Biopharmaceutics

journal homepage: www.elsevier.com/locate/ejpb

Research paper

Albumin-derived perfluorocarbon-based artificial oxygen carriers: A physico-chemical characterization and first *in vivo* evaluation of biocompatibility

Anna Wrobeln [a,1], Julia Laudien [a,1], Christoph Groß-Heitfeld [b], Jürgen Linders [b], Christian Mayer [b], Benjamin Wilde [d], Tanja Knoll [a], Dominik Naglav [c], Michael Kirsch [a], Katja B. Ferenz [a,*]

[a] University of Duisburg-Essen, Institute for Physiological Chemistry, University Hospital Essen, Hufelandstr. 55, 45122 Essen, Germany
[b] University of Duisburg-Essen, Institute for Physical Chemistry, CeNIDE, Universitaetsstr. 5, 45141 Essen, Germany
[c] University of Duisburg-Essen, Institute of Inorganic Chemistry, CeNIDE, Universitaetsstr. 5, 45141 Essen, Germany
[d] Department of Nephrology, University Hospital Essen, Hufelandstr. 55, 45122 Essen, Germany

ARTICLE INFO

Article history:
Received 1 September 2016
Revised 16 February 2017
Accepted in revised form 17 February 2017
Available online 20 February 2017

In commemoration of Herbert de Groot (Deceased May 10th, 2016)

Keywords:
Artificial oxygen carrier
Albumin
Blood substitutes
Intravenous administration
Nanocapsules
Nanoparticles
Perfluorocarbon
Perfluorodecalin

ABSTRACT

Until today, artificial oxygen carriers have not been reached satisfactory quality for routine clinical treatments. To bridge this gap, we designed albumin-derived perfluorocarbon-based nanoparticles as novel artificial oxygen carriers and evaluated their physico-chemical and pharmacological performance.

Our albumin-derived perfluorocarbon-based nanoparticles (capsules), composed of an albumin shell and a perfluorodecalin core, were synthesized using ultrasonics. Their subsequent analysis by physico-chemical methods such as scanning electron-, laser scanning- and dark field microscopy as well as dynamic light scattering revealed spherically-shaped, nano-sized particles, that were colloidally stable when dispersed in 5% human serum albumin solution. Furthermore, they provided a remarkable maximum oxygen capacity, determined with a respirometer, reflecting a higher oxygen transport capacity than the competitor Perftoran®. Intravenous administration to healthy rats was well tolerated. Undesirable effects on either mean arterial blood pressure, hepatic microcirculation (determined by *in vivo* microscopy) or any deposit of capsules in organs, except the spleen, were not observed. Some minor, dose-dependent effects on tissue damage (release of cellular enzymes, alterations of spleen's micro-architecture) were detected.

As our promising albumin-derived perfluorocarbon-based nanoparticles fulfilled decisive physico-chemical demands of an artificial oxygen carrier while lacking severe side-effects after *in vivo* administration they should be advanced to functionally focused *in vivo* testing conditions.

1. Introduction

Allogenic erythrocyte transfusions represent a life-securing intervention in modern medicine. However, the availability of erythrocyte concentrates (ECs) is limited and they are discussed critically because of potential infection risks and immunomodulation phenomena [1–3]. The implementation of restrictive transfusion triggers [1] as well as of more global measures called "patient blood management" [2] are still not sufficient to resolve the shortage of ECs, caused by the demographic change and the co-occurring declining willingness for blood donation of the population [4–6]. However, efficient supply of molecular oxygen (O_2) to the tissue with a simultaneous removal of carbon dioxide from the organism, is impaired not only in anemic or hemorrhagic

Abbreviations: ALAT, alanine aminotransferase; ASAT, aspartate aminotransferase; CK, creatine kinase; DAPI, 4′,6-diamidin-2-phenylindole; FITC, fluorescein isothiocyanate; ^{19}F-NMR, ^{19}F-nuclear magnetic resonance spectroscopy, HSA, human serum albumin; HSA, , human serum albumin; IVM, *intravital* microscopy; LDH, lactate dehydrogenase; LSM, laser scanning microscopy; MAP, mean arterial blood pressure; PFC, perfluorocarbon; PFD, perfluorodecalin; PI, polydispersity index; SEM, scanning electron microscopy; EC, erythrocyte concentrate; pO_2, pCO_2 oxygen and carbon dioxide partial pressure; RI, refractive index; Vis, viscosity; ANOVA, analysis of variance.

* Corresponding author.
E-mail addresses: anna.wrobeln@stud.uni-due.de (A. Wrobeln), julialaudien@gmx.de (J. Laudien), chrisgh@gmx.de (C. Groß-Heitfeld), christian.mayer@uni-due.de (C. Mayer), benjamin.wilde@uk-essen.de (B. Wilde), tanja.knoll@gmx.de (T. Knoll), dominik.naglav@uni-due.de (D. Naglav), michael.kirsch@uni-duisburg-essen.de (M. Kirsch), katja.ferenz@uk-essen.de (K.B. Ferenz).
[1] Contributed equally.

http://dx.doi.org/10.1016/j.ejpb.2017.02.015
0939-6411/

patients [1,7,8] but also at blood shortage scenarios [9]. In such situations, artificial oxygen carriers dispersed in plasma-like media would be an urgently awaited alternative to ECs. Most importantly, ECs change their physico-chemical qualities during storage while until today the consequences of those changes on patients as well as the optimal parameters of storage of ECs are still not defined unanimously [5,10]. Although artificial oxygen carriers are available in a couple of countries such as Russia, Ukraine, Mexico, Kyrgyzstan and Kazakhstan (Perftoran®, perfluorocarbon-based) [11,12] as well as South Africa and Russia (Hemopure®, hemoglobin-based) [13], authorities in Europe, Japan or USA still reject those drugs because of unbalanced risk-benefit analysis [13]. However, the use of perfluorocarbon-based artificial oxygen carriers is particularly attractive as perfluorocarbons (elsewise than hemoglobin-based drugs) may be used not only to bridge blood loss but also for therapy of decompression sickness [14,15] and smoke poisonings [16,17] as they remain functional even in the presence of flue gases, e.g. carbon monoxide. For intravenous use, perfluorocarbons must be processed to become compatible with the aqueous medium blood [18]. This is achieved either by emulsification or encapsulation [11,19–23]. However, both alternatives go along with various undesirable side-effects that have been attributed to biological incompatibility of the emulsifiers or to immune reactions against the synthetic polymers that have been used for encapsulation [19,22,24–27]. In contrast, the biopolymer albumin qualifies in particular for medical research purposes due to the absence of toxicity and antigenicity [28]. Because of the amphiphilic character of albumin, there is no need to introduce any additional emulsifier [29]. Albumin also appears in the context of artificial oxygen carriers; in fact in both classes: hemoglobin-based [30–32] and perfluorocarbon-based artificial oxygen carriers [33]. However, the perfluorocarbons used in the past led to severe side-effects [34] and exhibited excessively long organ retention (not tolerated by regulatory authorities) [11]. Meanwhile it is known, that other perfluorocarbons, e.g. perfluorodecalin (PFD) or perfluorooctyl bromide, show acceptable organ retention times and less severe side-effects [35,36]. This is why we combined for the first time the medical appropriate perfluorocarbon PFD with the most promising synthesis procedure (ultrasonics in the presence of albumin) resulting in albumin-derived perfluorocarbon-based artificial oxygen carriers (capsules). The present study was to conduct an *in vitro* characterization and first *in vivo* evaluation of the novel capsules to prove their feasibility for intravenous administration. Therefore, their physico-chemical properties including the absolute oxygen capacity as well as effects on blood viscosity were studied *in vitro*. Furthermore, effects of the capsules on acid base status, tissue damage, mean arterial blood pressure, hepatic microcirculation as well as their organ distribution were studied *in vivo*.

2. Materials and methods

2.1. Materials

5% human serum albumin solution (5% HSA, containing 5% human serum albumin, 0.75% NaCl, 0.11% sodium-N-acetyltryptophanoate, 0.07% sodiumcaprylate) was purchased from Baxter (Unterschleissheim, Germany). Perfluorodecalin (PFD) was from Fluorochem Chemicals (Derbyshire, UK), CASO Bouillon from Carl Roth (Karlsruhe, Germany), 1.5% agar from Merck (Darmstadt, Germany) and limulus amebocyte lysate reagent water from Lonza (Walkersville, MD, USA). NaCl (0.9%) was obtained from B. Braun (Melsungen, Germany). All other chemicals were purchased from Sigma Aldrich (Steinheim, Germany).

2.2. Synthesis of capsules

The synthesis of capsules was based on a method of Sloviter et al. [33]. In detail, 5 ml of 5% HSA and 1 ml PFD were combined in a reaction tube with a total capacity of 15 ml. The reaction tube was cooled in an ice bath and the mixture was sonicated for 90 s using a sonotrode with a tip diameter of 3 mm associated with a UP 400S ultrasonic processor (Hielscher, Teltow, Germany). For sonication the tip of the sonotrode was placed at the PFD–water interface. At a power of 400 W, ultrasonic amplitudes with 210 μm and a frequency of 24 kHz were generated. After synthesis, capsules were adjusted to 32 vol% or 64 vol% using micro-hematocrit glass capillary tubes (d = 1.15 mm, Brand, Wertheim, Germany) and a centrifuge (Universal 320R, Hettich, Tuttlingen, Germany) with a hematocrit rotor.

2.3. Scanning electron microscopy (SEM)

For SEM measurements, lager capsules (0.8 μm diameter) were synthesized, washed with and stored in purified H_2O (purified with a Milli-Q® Integral System from Merck Millipore).

For routine SEM, capsules, suspended in an aqueous solution, were fixed with 2.5% glutaraldehyde in purified H_2O for 30 min. After centrifugation, the specimens were dropped on poly-lysine covered glass slips, routinely dehydrated in a graded series of ethanol followed by critical point drying (CPD 7501, Polaron) and sputtered with platinum/palladium (208HR, Cressington). Capsules were analyzed in a Hitachi S-4000 SEM and images were obtained with a DISS5 (Point Electronics) analysis system.

2.4. Laser scanning microscopy (LSM)

For LSM procedure, capsules were synthesized using a combination of 90% HSA and 10% fluorescein isothiocyanate-labeled (FITC) HSA. Therefore, human albumin derived from rice was labeled with FITC and purified according to the method of Brookes and Kaufman [37]. To obtain larger capsules for better visualization the power of the sonotrode and the sonification time were reduced to 160 W and 30 s, respectively. A laser-scanning microscope (LSM 510, Zeiss, Oberkochen, Germany) equipped with an argon laser was used to study the capsules. The objective lens was a 100× NA 1.30 oil Fluar. Image processing and evaluation were performed using the software of the LSM 510 imaging system.

2.5. Flow cytometric analysis

The total number of capsules/μl equivalent to a 32 vol% capsule-dispersion was determined with flow cytometric analysis using FITC-labeled capsules. To that purpose, human albumin derived from rice was labeled with FITC and purified according to the method of Brookes and Kaufman [37]. FITC-HSA-spectrum was checked afterwards on a fluorometer (RF-1501, Shimadzu, Duisburg, Germany) before a mixture of HSA and FITC-HSA (9:1) was used for standard capsule synthesis (see above). Six different batches of FITC-labeled capsules (32 vol%) were produced, transferred into purified H_2O and measured in repeated determination. Flow cytometric data was acquired on a Navios cytometer (Beckman Coulter, Krefeld, Germany). Labeled capsules were detected in FL1 channel, each FITC-labeled event was considered as capsule. Proper controls were used for standardization. For quantitation and standardization purposes, Accu check counting beads were used (Invitrogen, Life Technologies, Darmstadt, Germany). Fifty μl of capsules (diluted 1:10 with purified H_2O) were mixed with 400 μl purified H_2O and 100 μl Accu check counting beads. Data was analyzed by using Kaluza Version 1.2 (Beckman Coulter).

2.6. Determination of the zeta potential, the polydispersity index and the capsule diameter

For the determination of the zeta potential, the capsule diameter and the polydispersity index (PI), six different batches of capsules were synthesized and washed, afterwards, with different media (0.9% NaCl, 5% HSA or purified H_2O) and then stored in the respective media at 4 °C until measurement (in duplicate) on day 1, 3 and 7 after synthesis. The size distribution and zeta potential measurements were performed with a Zetasizer ZS (Malvern Instruments, Zetasizer software Version 7.11.) in intensity mode, with a 173° angle (non-invasive backscattering) in a clear disposable zeta cell (Malvern DTS1070) at 25 °C. For the measurement, 50 µl of the capsules were diluted in 950 µl of the respective storage media. The refractive index (RI) of the capsule wall material albumin was 1.89 with an absorption of 0.01. The parameters (RI and viscosity (Vis)) of the different media (outer phases) were as follows: purified H_2O RI = 1.33, Vis 0.89 mPa s; 0.9% NaCl RI = 1.346, Vis 0.89 mPa s; 5% HSA RI = 1.345, Vis 1.25 mPa s.

2.7. Dark field microscopy

One day after synthesis, the colloidal stability of the capsules dispersed in different media (0.9% NaCl, 5% HSA, purified H_2O) was visualized by a dark-field microscope (Leitz Orthoplan with a 40× magnitude) and recorded with a CCD-camera (FireWire-Cam-011H, Phytec) [38].

2.8. Microbial long-term stability

Microbial long-term stability of capsules was assessed according to the European Pharmacopoeia in consideration of the guidelines for the testing for sterility of parenteral drugs [39]. Therefore, samples of capsule-dispersions were plated on agar plates containing CASO bouillon and 1.5% agar. Limulus amebocyte lysate reagent water served as negative control. Both, Limulus amebocyte lysate reagent water and capsule-dispersion were stored at 4 °C during the experimental period of 4 weeks. As a positive control intestine eluate extracted from rat intestine was used. The plating was performed under aseptic conditions (except for positive control) twice a week over a period of 4 weeks starting at the day of capsules synthesis. Plates were incubated for 72 h at 37 °C before they were evaluated macroscopically with regard to an up growth of microbial colonies.

2.9. Influence on hemorheology

The measurements of the dynamic blood viscosities were carried out by a rotational viscometer "Low Shear 40" from proRheo and a DIN 412 Coutte measurement system. To check effects of capsules and dispersion media on hemorheology, capsules in different media (washed and stored in 0.9% NaCl or washed and stored in 5% HSA) were diluted with human blood in a therapeutically relevant concentration (1:7.2). Human blood of six healthy controls was used after obtaining informed consent (IRB number 13-5500-BO). The data for the NaCl graph was recorded with 0.9% NaCl diluted with blood (1.7.2); the 5% HSA graph with 5% HSA in blood (1:7.2). Six fold measurements were done for all samples except for pure blood (each of the six samples was measured only one fold) at shear rates from 1 to 100 rad s^{-1} and 37 °C. Before each measurement, the sample was equilibrated for 1 min to obtain the desired temperature.

2.10. Oxygen capacity of capsules

To determine the therapeutically relevant oxygen capacities of the capsules, oxygen content of capsule-dispersions was discovered using a respirometer (Oxygraph-2k, oroboros instruments, Innsbruck, Austria). Measurement error correction was performed prior to each test series. Therefore, measuring chambers of the oxygraph were filled with a total amount of 2 ml water and tempered to 37 °C. Water was stirred and incubated at atmospheric pressure until constant oxygen content was reached. Based on this maximum value in oxygen content and on the theoretical oxygen capacity of water under the given terms (209 nmol/ml), the correction factor $F(O_2)$ was calculated as followed:

$$F(O_2)\ [\mathrm{mmol/ml}] = \frac{\text{max. } O_2\text{content}_{H_2O}(\text{set})}{\text{max. } O_2\text{content}_{H_2O}(\text{actual})}$$

Measuring chambers were filled with phosphate buffer (50 mM) and hermetically sealed. Oxygen resolved in buffer was removed by adding 96 µl yeast (83 mg/ml in phosphate buffer) and 50 µl glucose (1 M in phosphate buffer). Subsequently, 60 µl potassium cyanide (100 mM in phosphate buffer) were added to prevent aerobic metabolism of the yeast in the processing experiment.

To ensure oxygen charging of the capsule-dispersions, a reaction vessel was sealed using a *septum* and flushed with pure oxygen for a minute to maintain an absolute oxygen atmosphere. Subsequently, 2 ml of capsule-dispersion or 5% HSA were injected into the reaction vessel and incubated at 37 °C in pure oxygen atmosphere while stirring. By subtracting the water vapour pressure (≈47 mmHg) from the pure oxygen partial pressure (pO_2) (≈760 mmHg) an existing pO_2 of 713 mmHg could be calculated for the reaction tube. After oxygen loading, 50 µl of capsule-dispersion or 5% HSA were applied to the oxygen-free measuring chambers of the Oxygraph 2-k under exclusion of air. The maximum amount of oxygen off-loading was read off and the maximum oxygen capacity of capsules and control group was calculated by taking the correction factor into consideration. Oxygen capacity was given in ml/dl. As the determined oxygen capacities displayed the overall amount of capsules and medium, the oxygen capacities of the capsules was calculated under consideration of the volume distribution with x = volume percentage of media in capsule dispersion.

$$O_2\text{fraction}_{\text{medium}}\ [\mathrm{ml/dl}] = O_2\text{capacity}_{\text{medium}} \times \frac{X}{100}$$

$$O_2\text{content}_{\text{capsules}}\ [\mathrm{ml/dl}] = O_2\text{capacity}_{\text{capsule dispersion}} \times O_2\text{content}_{\text{medium}}$$

2.11. Animals

A total number of 43 male Wistar rats (*Rattus norvegicus*, 400–450 g) were obtained from the central animal unit of the University Hospital Essen. Animals were kept under standardized temperature conditions (22 ± 1 °C), humidity (55 ± 5%) and 12/12-h light/-dark cycles with free access to food (ssniff-Spezialdiaeten, Soest, Germany) and water. All animals received humane care according to the standards of Annex III of the directive 2010/63/EU of the European Parliament and of the Council of 22 September 2010 on the protection of animals used for scientific purposes [40]. The experimental protocol was approved by the North Rhine-Westfalia state office for Nature, Environment and Consumer Protection (Landesamt fuer Natur, Umwelt und Verbraucherschutz Nordrhein-Westfalen), Germany, based on the local animal protection act.

2.12. Anesthesia, analgesia, and surgical procedure

Rats were anesthetized with isoflurane (2.0% in 100% medical O_2 at 4.0 l/min for induction, 1.5–2.0% isoflurane in 100% medical O_2 at 1.0 l/min throughout the experiment) through face masks connected to a vaporizer (Isofluran Vet. Med. Vapour; Draeger, Luebeck, Germany). For analgesia they received ketamine subcutaneously (50 mg/kg body weight) into the right chest wall. After local lidocaine administration (5 mg/kg body weight subcutaneously), a median skin-deep inguinal incision of about 2 cm was made along the right groin and a Portex catheter (0.58 mm ID, 0.96 mm OD) was placed within the right femoral artery and the right femoral vein. Each catheter was fixed with a surgical suture. At the end of experiment, animals were sacrificed by resection of the heart, liver, spleen, lung, kidney, brain, *musculus gastrocnemius* and small intestine under deep isoflurane anesthesia.

2.13. Biomonitoring

Systolic blood pressure, diastolic blood pressure and mean arterial pressure (MAP) were recorded continuously via the femoral artery catheter. The catheter was connected to a pressure transducer and blood pressure was displayed on a monitor. Heart rates were determined from systolic blood pressure spikes and breathing rates were calculated by counting the ventilation movements per minute every 10 min. The body core temperature of the rats was continuously monitored using a rectal sensor. A cooling below 37 °C was prevented by an underlying thermostat-controlled operating table as well as by covering the animals with wrapping film. With a special device (oxygen to see (O2C), Lea medical engineering, Giessen, Germany) local oxygen supply (sO2), blood flow, as well as blood flow velocity of the *musculus gastrocnemius* were measured pre- and post-infusion as well as 60 and 120 min post infusion.

2.14. Assessment of blood and plasma parameters

Blood samples (0.5 ml) for blood gas analysis as well as for the monitoring of enzyme activities in plasma were taken from the femoral artery catheter directly after catheterization of *A. femoralis*, 30 min before initiation of infusion and subsequently 30, 60, 90, 120, 150 and 180 min after start of the infusion using a 2 ml syringe containing 80 IU electrolyte-balanced heparin (Pico50, Radiometer Medical, Brønshøj, Denmark). For each blood sampling, animals were substituted with a 0.5 ml bolus of 0.9% NaCl solution via the femoral artery (with the additional effect to keep the catheter functional). In order to obtain plasma, blood was centrifuged at 4500*g* for 10 min at room temperature. The gained plasma was used straightaway for the determination of the activity of released enzymes.

2.14.1. Blood gas analysis

Arterial blood pH, oxygen and carbon dioxide partial pressures (pO_2, pCO_2), base excess (BE), bicarbonate and lactate were assessed with a blood gas analyzer (ABL 715, Radiometer, Copenhagen, Denmark).

2.14.2. Enzyme activities

The plasma activity of lactate dehydrogenase (LDH) as a general marker of cell injury, creatine kinase (CK) as a marker for muscle cell injury, aspartate aminotransferase (ASAT) and alanine aminotransferase (ALAT) as markers for hepatocyte injury as well as the plasma creatinine concentration as a marker of renal function were determined using a fully automated clinical chemistry analyzer (Vitalab Selectra E, VWR International, Darmstadt, Germany) using commercially available reagent kits (DiaSys, Holzheim, Germany).

2.15. Assessment of microcirculation and physiological functions

2.15.1. In vivo microscopy

In vivo fluorescence microscopy analysis (IVM) of the left lateral liver lobe was performed as described previously [22]. A study group receiving 32 vol% capsules (20 ml/kg body weight × h) was compared to a group receiving 5% HSA (20 ml/kg body weight × h). To exclude any effects of albumin, a second control group received 0.9% NaCl (20 ml/kg body weight × h). Each group consisted of 6 animals. The following parameters were determined in five randomly selected acinar areas and post sinusoidal venules:

1. Vessel diameters of sinusoids and post sinusoidal venules were defined by image analysis software (Kappa ImageBase 2.8.2.11051, Kappa Optronics GmbH, Gleichen, Germany).
2. The number of perfused sinusoidal vessels (the ratio of perfused sinusoids to all sinusoids visible in a defined acinar area) (%) was determined by analyzing full video sequences by an examiner blinded to the experimental groups.

2.15.2. Frozen section procedure

In order to evaluate the *in vivo* distribution of the capsules, cryosections of liver, spleen, lung, kidney, brain, heart, *M. Gastrocnemius* and small intestine were prepared 40 min after administration of 32 vol% FITC-labeled capsules (20 ml/kg body weight × h, see Section 2.4 for preparation) as described previously [22]. The study group consisted of 3 animals.

2.16. Determination of the circulatory in vivo half-life of the capsules

After administration of 32 vol% capsules (20 ml/kg body weight × h) blood samples were taken from the femoral artery directly at the end of infusion and subsequently 60, 120 and 180 min after the end of infusion. Samples were stored at −80 °C until further analysis by ^{19}F-nuclear magnetic resonance spectroscopy (^{19}F-NMR) and the total amount of PFD within the samples was calculated as described previously [22]. The study group consisted of 3 animals. We assumed a virtual IV bolus model and assumed the intravascular capsule concentration at the time point $t_{30min} = t_{max}$ to be c_{max}.

2.17. Histological evaluation of spleen, liver and kidney

For histological examinations spleen, kidney and liver were resected as described previously [22]. Paraffin-embedded sections were stained with hematoxylin-eosin and evaluated in a blinded manner (5 image sections per tissue section). Spleen sections were assessed for integrity of red and white pulp. Kidney sections were assessed by scanning the renal tubules for vacuoles and the integrity of cell membranes and epithelium as well as by examining the glomeruli for swelling or shrinkage. Liver sections were assessed for integrity and vacuolization. All organ sections were investigated by light microscopy with a magnification of ×200.

Spleen macrophages were stained as described previously using a primary antibody against the antigen ED:1 (diluted 1:1000 in PBST, BIOLOGO, Kronshagen, Germany) [41]. The relative area (%) of stained macrophages in each spleen was quantified (magnification of ×400, 5 image sections per spleen) using light microscopy and ImageJ2 version 1.5.1; the results were presented in a bar chart. For an overview of the spleen, images with a magnification of ×100 of representative spleen sections with an insert of an image with a magnification on ×400 were displayed.

2.18. Statistical analysis

Data are expressed as mean values ± SD for *in vitro* experiments and ±SEM for *in vivo* experiments. Comparisons among multiple groups were performed using two-way analysis of variance (ANOVA) for repeated measurements followed by Dunnett post hoc analysis (Figs. 3, 5–7 and S2) or a one-way ANOVA followed by Dunnett post hoc analysis (Fig. 4). A p-value <0.05 was considered to indicate significance. Two-way ANOVA of LDH activity in plasma (Fig. 6D) was done with n = 5 for 64 vol% capsules and n = 6 for 5% HSA and 32 vol% capsules, respectively. For statistical analysis of the circulatory *in vivo* half-life (Fig. 9) we performed an exponential one-phase decay least squares ordinary fit based on the following equation:

$$Y = (Y0 - plateau) \times \exp(-K \times X) + plateau$$

The half-life was calculated with ln(2)/K. For every statistical analysis, graph pad prism 6.05 (Graph Pad Software Inc., La Jolla, CA, USA) was used.

3. Results and discussion

3.1. Selection of the appropriate preparation method

There exist several methods for the preparation of albumin particles, e.g. thermal or chemical stabilization [28]. For synthesizing albumin nanoparticles by thermal stabilization temperatures of 175–180 °C must be applied [28]. As perfluorodecalin displays a boiling point of 142 °C, this technique is not feasible for perfluorodecalin-filled particles. Additionally, all albumin molecules present in the formulation would be cross-linked; not only those forming the perfluorodecalin-filled capsules but also those dissolved in the surrounding medium. Therefore, using this method capsules cannot be produced directly in the favored dispersion medium but only in protein-free solution and must be transferred afterwards into plasma-like dispersion media (containing free albumin molecules). This requires either subsequent centrifugation steps (maybe triggering capsule agglomeration) or subsequent enrichment with albumin; both undesired additional production steps. In contrast to thermal stabilization, chemical stabilization can be performed at room temperature but always involves harmful chemicals such as glutaraldehyde being responsible for side effects during *in vivo* use. Furthermore, chemical stabilization entails the same problems concerning dissolved free albumin molecules as thermal stabilization does. Because it is known that ultrasound irradiation at the interface of an aqueous protein solution and a nonpolar liquid results in proteinaceous microspheres at high concentrations with a narrow size distribution [42], we applied this method utilizing aqueous albumin solution in combination with the nonpolar liquid perfluorodecalin. Thereby, only albumin molecules located at the albumin/perfluorodecalin interface (thus albumin molecules forming the capsule shell) should be cross-linked [28,42]. The three-dimensional structure of the capsules was verified by SEM and LSM measurements, respectively. Capsules showed a spherical hollow shape (Fig. 1). Furthermore, as expected, the used preparation method resulted in a dispersion of discretely distributed perfluorodecalin-filled albumin-based capsules (Fig. 1). The 32 vol% of the capsule-dispersion was equivalent to about 8×10^7 capsules/ml as determined by fluorescence-activated cell sorting analysis. Notably this preparation technique (ultrasonics) had been successfully applied to other perfluorocarbons (perfluorononane [42] and a mixture of perfluorobutyltetrahydrofuran and perfluorotributylamine [33]).

Due to the fact that ultrasonic contributes to devitalize bacteria and allows therefore to work under aseptic conditions with sterile raw materials, this procedure represents an ideal preparation method for albumin capsule dispersions designed for *in vivo* use. As a consequence of ultrasonic-depending bacterial killing, microbial long-term stability assay revealed that capsule dispersions were free of any microbial growth sign within 4 weeks after capsule preparation (Fig. S1). Of course, this further supported the good suitability of the chosen method for the preparation of the novel albumin-derived artificial oxygen carriers intended for intravenous use.

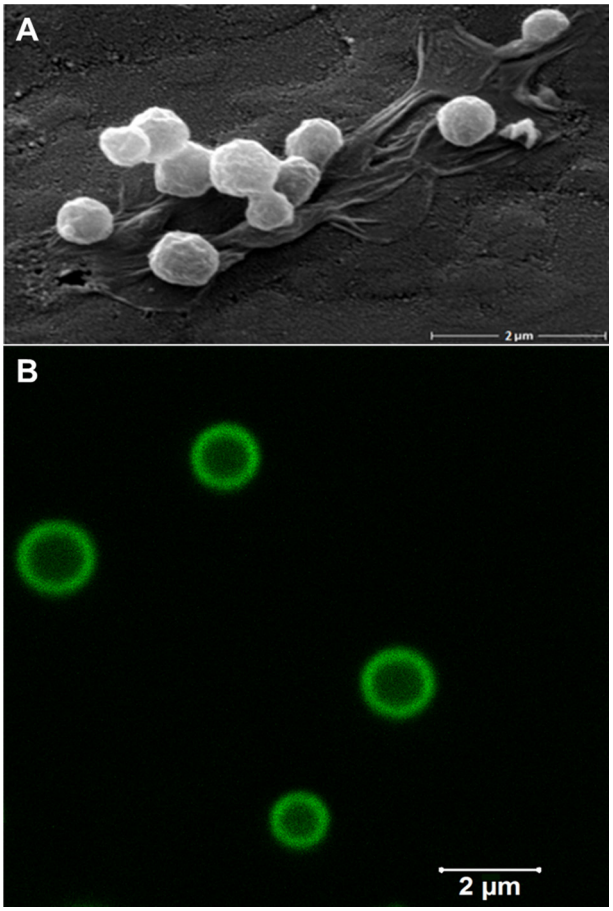

Fig. 1. Capsules' shape. The capsules' shape was recorded with (A) SEM, magnification 15,000× and (B) LSM magnification 8000×.

3.2. Influence of size and surface charge

After intravenous administration, particles are eliminated from the vasculature by the reticulo-endothelial system. Particles holding a size of 1–3 µm (the largest being eliminated first) were rapidly removed, so that artificial oxygen carriers should not exceed a diameter of 1 µm in general [32,35]. Apart from the synthesis procedure the selection of the proper raw material, e.g. type of perfluorocarbon and surfactant, is decisive for the particle size initially obtained [43]. In fact, using perfluorodecalin, nano-scale emulsions can be synthesized [43], but molecular diffusion and coalescence quickly lead to enlargement of emulsion droplets [35,44]. Nevertheless, the preparation of an apparently stable dispersion of nano-sized perfluorodecalin-filled capsules was achieved and importantly, the mean diameter of all preparations never exceeded 1 µm (Fig. 2). The signals at about 8 µm were considered to be artifacts. All animals survived the infusion of the capsule preparation and did not show any decrease in blood pressure (3.5).

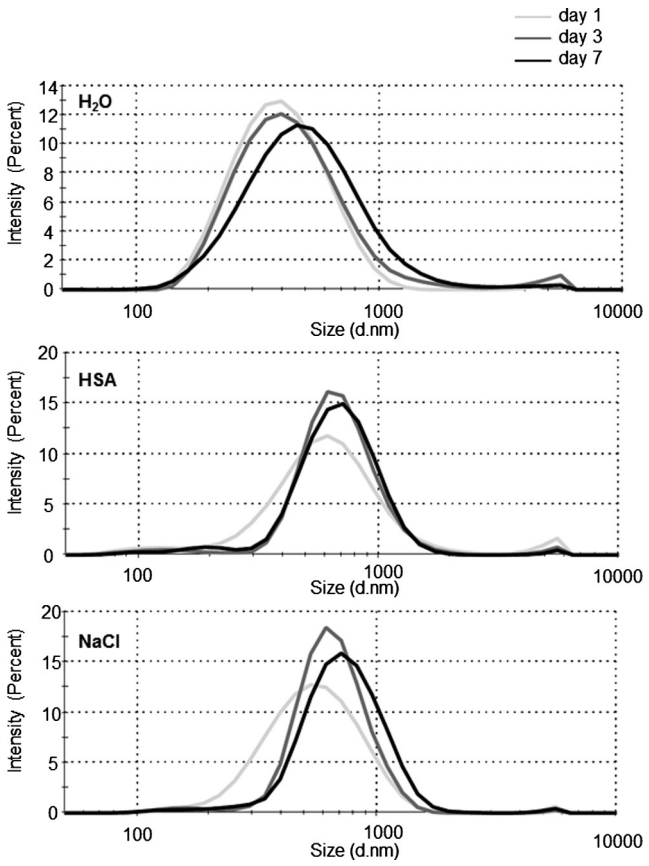

Fig. 2. Effect of storage media and storage time on capsule diameter. After synthesis, capsules were washed with and stored in different media (H_2O, 0.9% NaCl, 5% HSA) and the diameter was determined at the times indicated in repeated measurements after sample dilution with the particular medium.

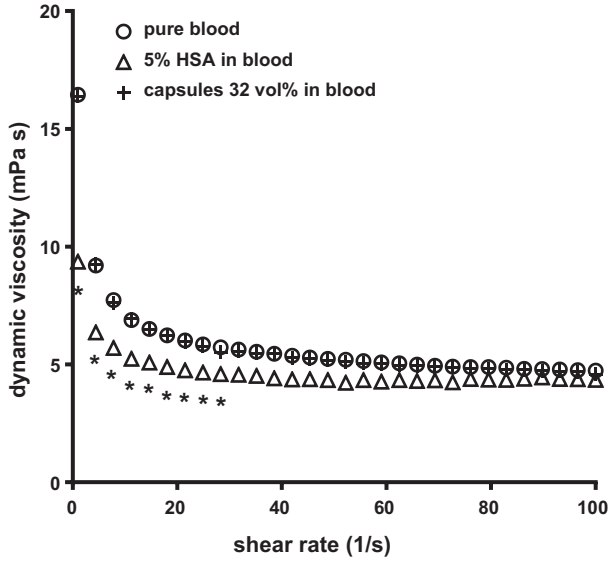

Fig. 3. Effect of capsule dispersion and 5% HSA on blood viscosity. The viscosity of capsules dispersed in 5% HSA as well as the viscosity of pure 5% HSA (all samples diluted with blood (1:7.2)) was measured and compared to pure blood, * $p < 0.05$.

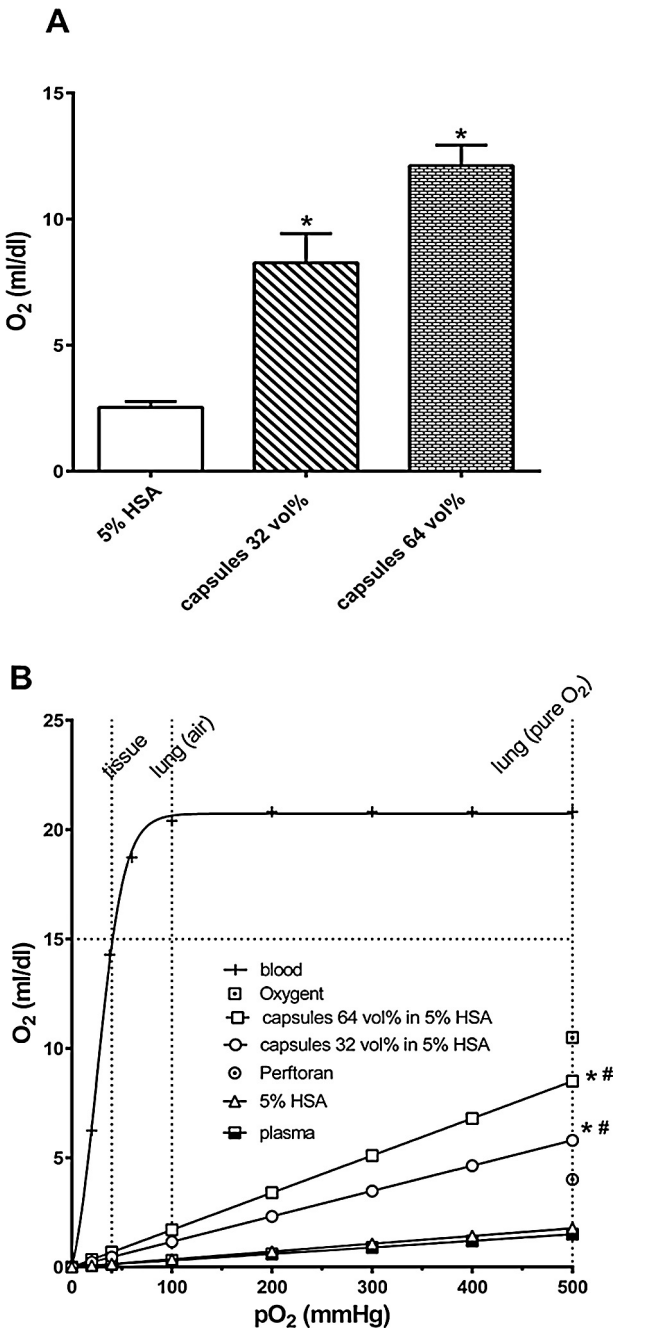

Fig. 4. Capsule's oxygen transport capacity. Oxygen transport capacities of pure 5% HSA and of different capsule concentrations (32 and 64 vol%) in 5% HSA were measured at pO_2 = 713 mmHg (A) and interpolated to physiologically relevant pO_2 (pO_2 tissue, pO_2 $lung_{air}$, pO_2 $lung_{pureO2}$) as well as correlated with oxygen transport capacity of blood, plasma and relevant perfluorocarbon emulsions (Oxygent® and Perftoran®, data obtained from[1]) (B). For better clarity, oxygen capacities of Oxygent® and Perftoran® are plotted only for pO_2 = 500 mmHg. Capsule dispersion compared to 5% HSA, * with $p < 0.0001$ at pO_2 = 713 mmHg (A) and pO_2 = 500 mmHg (B), and compared to Perftoran®, # with $p < 0.0001$) at pO_2 = 500 mmHg.

However, looking more closely on the different capsule dispersions (in water (H_2O), 0.9% NaCl, 5% HSA), differences in particle size and zeta potential attracted attention (Fig. 2 and Table 1). It is known, that both parameters are influenced by components present in the dispersion medium such as salt or proteins [45]. The smallest capsules (422 nm) were obtained in H_2O, whereas capsules in 0.9% NaCl showed a mean diameter of 588 nm. The largest capsules were formed in 5% HSA (707 nm) (Fig. 2). Thus, in accordance with data from Lochmann et al., it was observed that electrolytes triggered capsule agglomeration whereas free albumin molecules can stabilizes nanoparticle dispersions in the presence of salt [45]. Importantly, the mean particle diameter of capsules

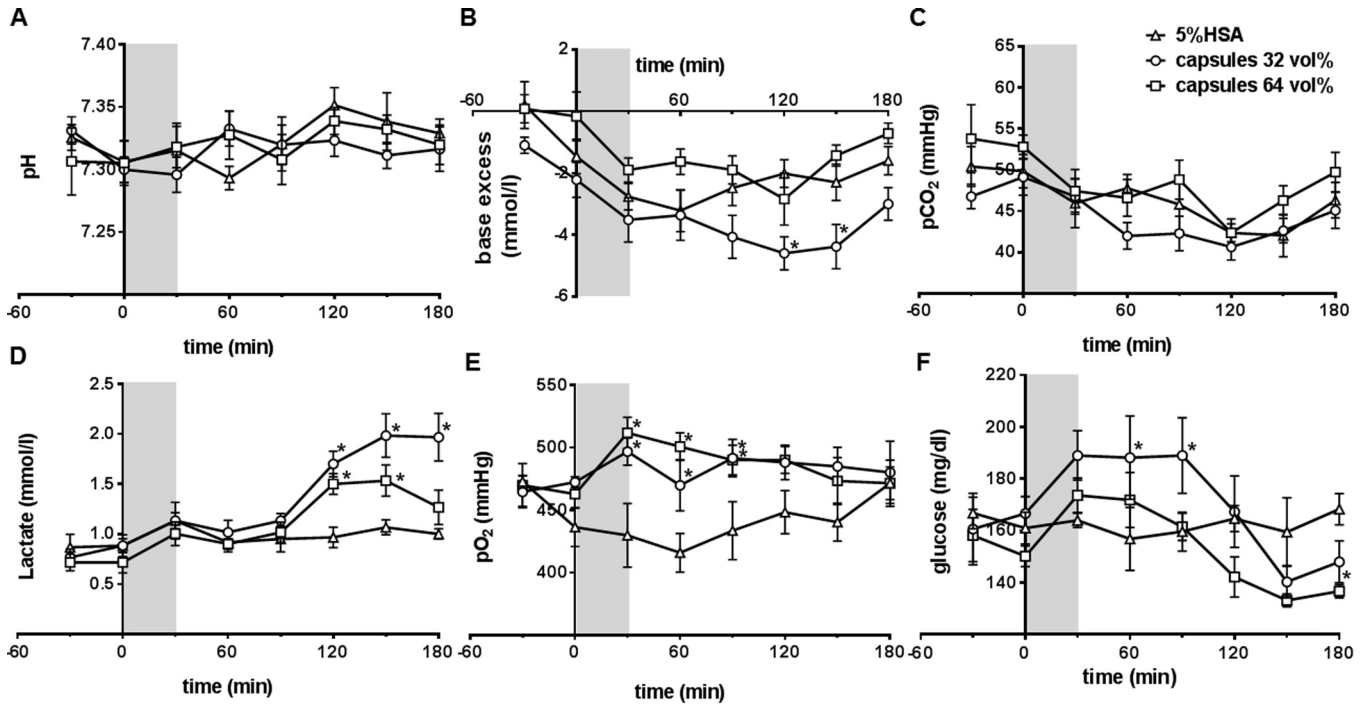

Fig. 5. Effects of capsule infusion on the acid base status: pH (A), base excess (B), pCO_2 (C), lactate (D), pO_2 (E) and glucose (F). Capsules or 5% HSA were infused over a period of 30 min (grey, 20 ml/kg body weight × h). The values plotted are mean ± SEM of 6 individual experiments per group, * $p < 0.05$ compared to 5% HSA group.

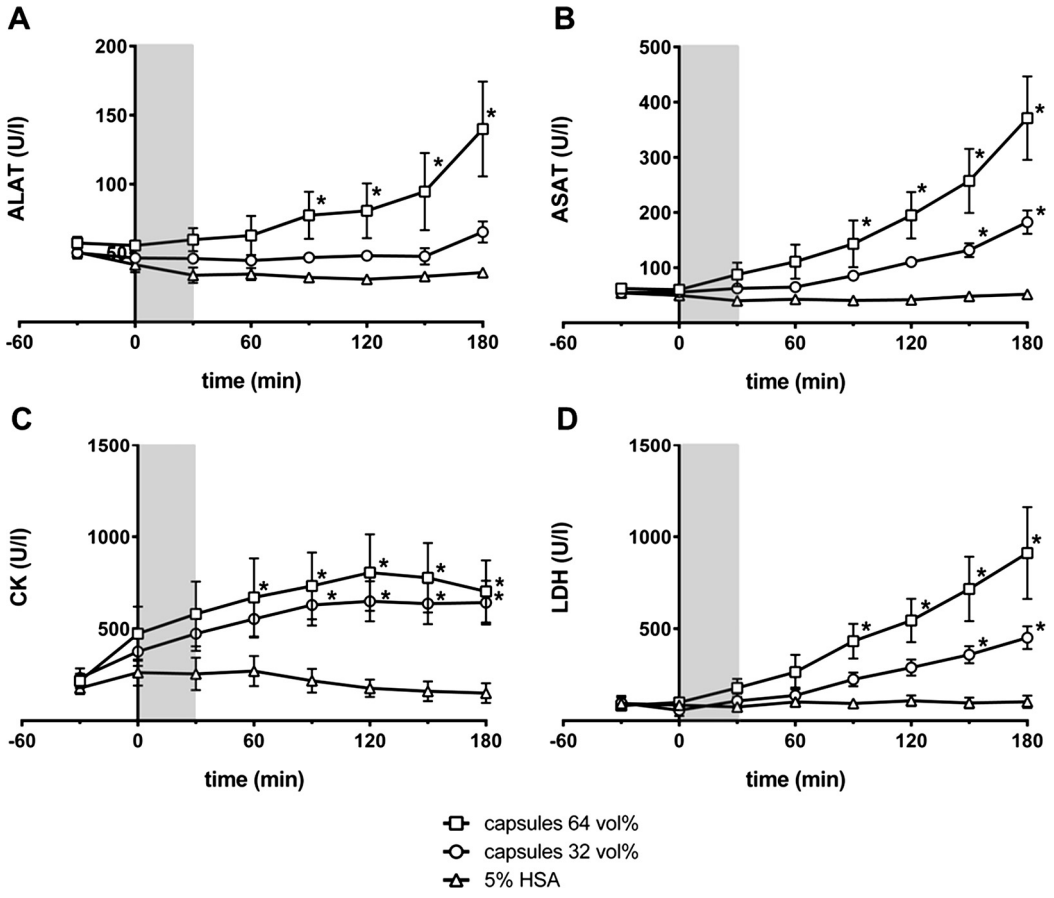

Fig. 6. Effects of capsule infusion on organ/tissue damage: creatinine (A), lactate dehydrogenase (LDH) (B), creatine kinase (CK) (C) and aspartate aminotransferase (ASAT) (D). Capsules or 5% HSA were infused over a period of 30 min (grey, 20 ml/kg body weight × h). The values plotted are mean ± SEM of 6 individual experiments per group, * $p < 0.05$ compared to 5% HSA group.

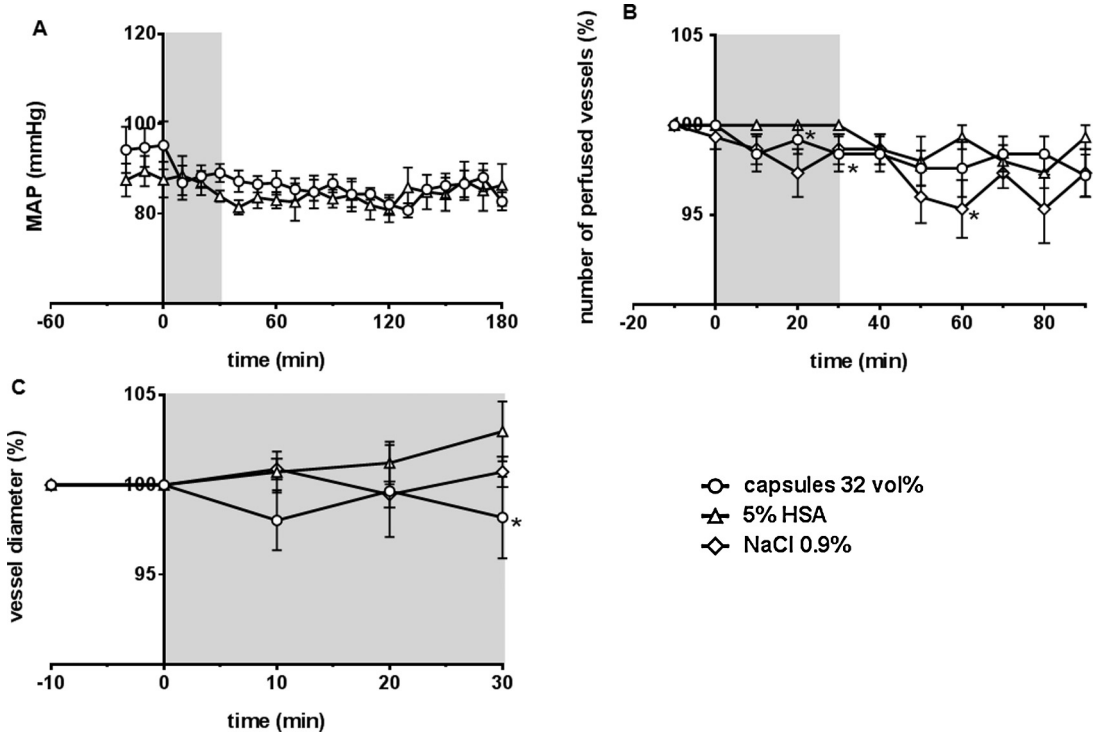

Fig. 7. Effects of capsule infusion on mean arterial blood pressure (A), hepatic perfusion rate (B) and hepatic vessel diameter (C): Capsules or 5% HSA were infused over a period of 30 min (grey, 20 ml/kg body weight × h). The values plotted are mean ± SEM of 6 individual experiments per group, * $p < 0.05$ compared to 5% HSA group.

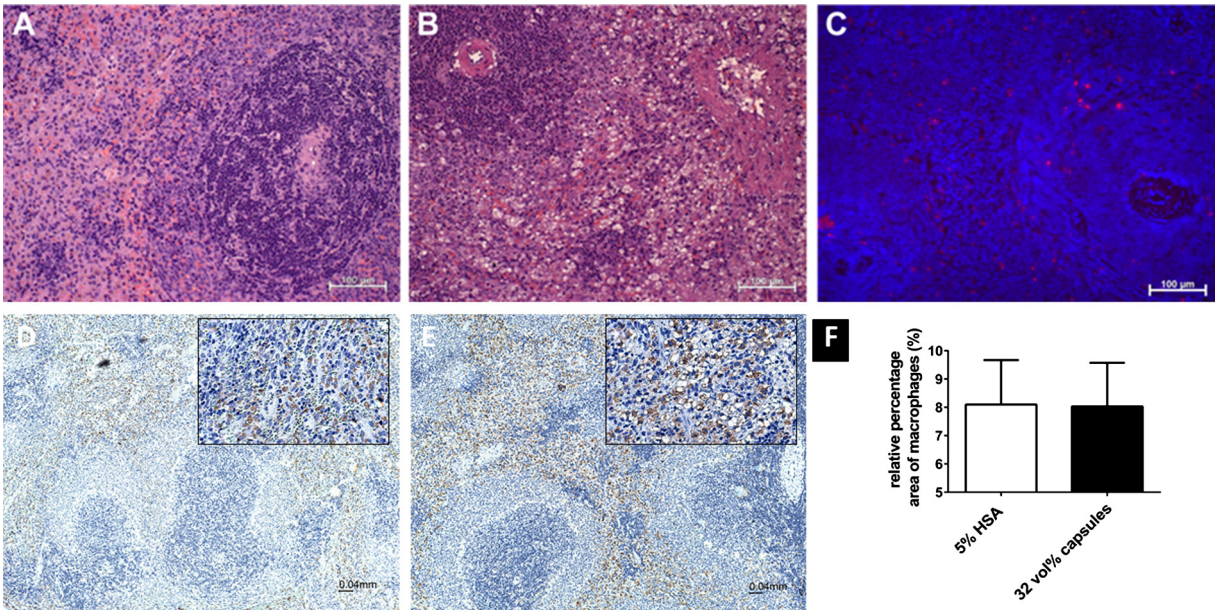

Fig. 8. Effects on tissue damage (A–B), organ distribution (C) and macrophages (D–F) of capsules 32 vol%. Microscopic assessment of haematoxylin-eosin stained organ tissue sections (magnification ×200) showed distinct changes in the organ architecture of the spleen after infusion of capsules (B) if compared to infusion of 5% HSA (A). Cryosections (magnification ×200) of the spleen (C) revealed accumulation of capsules (red). Nuclei were stained with 4′,6-diamidin-2-phenylindol (DAPI) (blue). Macrophage staining of spleen macrophages (magnification ×100 and ×400) showed unaffected macrophages after infusion of 5% HSA (D) in contrast to foamy vacuolized macrophages after infusion of capsules 32 vol% (E). The relative percentage area of macrophages of 6 individual experiments per group was presented + SD (F).

dispersed in 5% HSA (more physiological situation: electrolytes + albumin) remained nearly constant (Fig. 2). However, this medium originated the capsule dispersion with the broadest size distribution (polydispersity index (PI) of about 0.6, compared to a PI of 0.3 for capsules in H_2O and in 0.9% NaCl, respectively, Table 1).

The influence of the dispersion medium on capsule stability is also reflected in the zeta potential. A dispersion is colloidal stable, if repulsive electrostatic forces predominate attractive van der Waals forces [46]. During storage or, at the latest from intravenous injection, capsules will be exposed to cations, anions and nonionic-

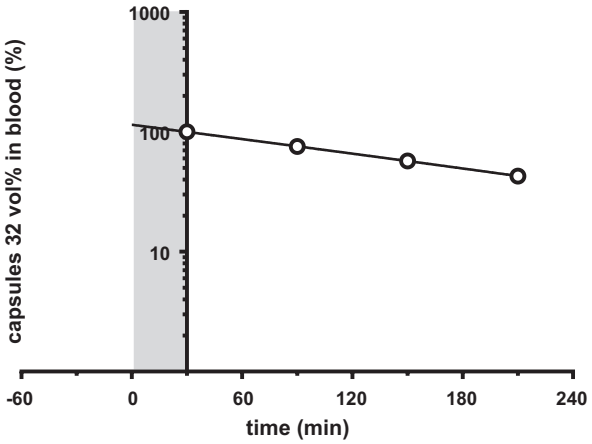

Fig. 9. *In vivo* half-life of capsules 32 vol%: The percentage of capsules in blood was calculated over a time period of 180 min post infusion by means of the total amount of PFD within the blood samples of the different time points. For better orientation, the infusion period (grey background) is also given. The values plotted are mean ± SEM of 3 individual experiments and are subjected to an exponential one phase decay least squares ordinary curve fitting, t_{max} = 30 min and c_{max} = 100%.

Table 1
Effects of storage media and storage time on capsule stability. After synthesis, capsules were washed with and stored in different media (H_2O, 0.9% NaCl, 5% HSA) and their zeta potential and polydispersity index determined at the times indicated in repeated measurements after sample dilution with the particular medium. Standard deviations (n = 6) are presented in parentheses.

	Zeta potential (mV)	Polydispersity index
1 day after synthesis		
Capsules in H_2O	−29.15 (3.68)	0.257 (0.17)
Capsules in 0.9% NaCl	−7.58 (0.85)	0.290 (0.04)
Capsules in 5% HSA	Non applicable	0.562 (0.05)
3 days after synthesis		
Capsules in H_2O	−18.43 (1.89)	0.234 (0.05)
Capsules in 0.9% NaCl	−7.73 (0.67)	0.230 (0.12)
Capsules in 5% HSA	Non applicable	0.650 (0.10)
7 days after synthesis		
Capsules in H_2O	−17.08 (2.90)	0.225 (0.06)
Capsules in 0.9% NaCl	−6.78 (0.39)	0.299 (0.08)
Capsules in 5% HSA	Non applicable	0.624 (0.14)

molecules influencing the zeta potential. Thus, electrostatic repulsive forces are mainly altered whereas van der Waals forces are not very sensitive to changes in electrolyte concentrations [46]. Interestingly, erythrocytes in blood start to aggregate at about <15 mV [46], although generally, good electrostatic stabilization is obtained if zeta potentials show a magnitude of >30 mV (ideally >60 mV). Our study showed capsule agglomeration in the presence of electrolytes that can be explained by the low zeta potential of about −8 mV (Table 1). If water was used as dispersion medium, the capsule dispersion initially seemed stable displaying a zeta potential in the same range as other albumin nanoparticles in water (about −30 mV) [47], but over time, the zeta potential was nearly halved, resulting in an unstable dispersion (Fig. 2 and Table 1). Although the measurement of the zeta potential of the capsules failed in 5% HSA or plasma due to technical limitations (the utilized instrument (Zetasizer ZS) calculates the zeta potential of particles based on laser-doppler micro-electrophoresis data), one might assume, that the shielding effect of free albumin molecules (as discussed below) originates a stable dispersion in that case (Fig. 2). This hypothesis can be substantiated by dark field microscopy measurements: Colloidal stability of capsules was good in H_2O and 5% HSA but disappointing in 0.9% NaCl, again confirming the aggregation of the capsules in a protein-free saline medium (see Supplemental videos 1–3). During storage, capsule diameter increased significantly from day 1 to day 7 if capsules were stored in 0.9% NaCl or H_2O but their diameters remained nearly constant, when capsules were kept in 5% HSA (Fig. 2). While initially, particles in H_2O were quite small and narrow-sized (Fig. 2), particle growth over time was probably caused by molecular diffusion, as the standard deviation of the diameter of the capsules increased by increasing the observation period which is characteristic for that process (Fig. 2). In contrast, free albumin molecules (if present in the medium) prevent capsule aggregation by absorbing to the capsules' surface before capsule aggregation can occur, because the diffusion of free albumin molecules is much faster than the one of the capsules [28]. This effect (amplified by other large macromolecules such as fibronectin or polysaccharides) will become particularly important when mixing the capsules with blood during *in vivo* use. The negative surface charge of the capsules due to the low isoelectric point of albumin [48] might be advantageous for low phagocytic uptake during *in vivo* use [47].

3.3. Effects on hemorheology

The influence of the capsule dispersion on blood viscosity was tested for different dispersion media. This is especially important as tissue ischemia can be caused by increased blood viscosity via the impairment of blood flow in the microvasculature [49]. Among the factors affecting blood viscosity, plasma proteins play a major role [49]. Furthermore, pure 5% HSA and pure 0.9% NaCl are Newtonian fluids which means that their viscosity is independent of the shear rate applied [30]. Therefore, after dilution of human blood with pure 5% HSA or pure 0.9% NaCl (without capsules), dynamic blood viscosity was significantly decreased, especially at lower shear rates (Figs. 3 and S2). In contrast, the non-Newtonian flow characteristics of blood were not affected when blood was mixed with capsule dispersion in physiologically relevant (see below) concentration. This was independent of the dispersion medium (Figs. 3 and S2) and is in line with data obtained for other perfluorodecalin-filled nanocapsules [22]. Similar tests with a hemoglobin-based artificial oxygen carrier dispersed in a medium containing 5% human serum albumin [30] (like 5% HSA used in the experiments presented here, Figs. 3 and S2) showed comparable results if considering the different dilution ratios (artificial oxygen carrier: blood).

3.4. Oxygen capacity

The oxygen capacity is an important parameter characterizing an artificial oxygen carrier. Their high oxygen solubility of 40–60 ml/dl [35] predestines perfluorocarbons as suitable raw materials for the preparation of artificial oxygen carriers [19,22,50,51]. As the oxygen solubility linearly depends on the partial oxygen pressure (pO_2), the potential of perfluorocarbons is tapped, not until their use is combined with high pO_2 [15]. Therefore, in the *in vitro* assay, capsules were aerated with pure oxygen resulting in a pO_2 of 713 mmHg. Because 5% HSA and blood plasma are comparable with respect to their oxygen capacity, the reliability of our assay was confirmed as the calculated oxygen solubility for 5% HSA (0.35 ml O_2/dl) under physiological conditions (breathing air, arterial pO_2 = 100 mmHg) matched the theoretical oxygen capacity of pure blood plasma (0.3 ml/dl). As expected, *in vitro* measurements of the oxygen capacities of the capsule dispersions revealed that albumin capsules dispersed in 5% HSA store more oxygen than pure 5% HSA (8.3 ml O_2/dl ± 1.2 ml O_2/dl for 32 vol% capsules in 5% HSA versus 2.5 ml/dl ± 0.2 ml O_2/dl for pure 5% HSA, Fig. 4A). In addition, the oxygen capacity was directly proportional to the amount of capsules being dispersed. The oxygen capacity of the

Table 2
Oxygen capacities of the perfluorocarbon-filled albumin-based capsule dispersions with different volume fractions (32 and 64 vol%) itemized by contribution of pure capsules and pure medium at a pO_2 of 713 mmHg.

	Total oxygen capacity of capsule dispersion (ml O_2/dl)	Oxygen capacity of pure capsules (ml O_2/dl)	Oxygen capacity of pure medium (ml O_2/dl)
32 vol%	8.3	6.6	1.7
64 vol%	12.1	11.2	0.9

pure capsule fraction of the 32 vol% dispersion was calculated to be 6.6 ml/dl while the pure capsule fraction of the 64 vol% dispersion displayed a calculated oxygen capacity of 11.2 mg/dl (Table 2).

In order to top out the maximum oxygen capacity of perfluorocarbons feasible under *in vivo* conditions, patients must be ventilated with pure oxygen instead of air thereby reaching an arterial pO_2 of up to 500 mmHg [52] (Fig. 4B). Under those conditions the oxygen capacity of an EC (containing 60% functional intact erythrocytes extracted from ~500 ml whole blood [53]) exceeds that of whole blood (hemoglobin content of 15 g/dl) by the factor 1.33, whereas the absolute oxygen capacity of perfluorocarbon-filled albumin-based capsules (64 vol%) only corresponds to less than half of the oxygen capacity of whole blood (15 g/dl, Table 3).

However, when talking about efficient oxygen supply of tissues, the maximal oxygen capacity is not what matters most. Irrespective of the fact, that a hemoglobin concentration of only 5 g/dl (equals 6.7 ml O_2/dl) is sufficient for survival [54], the oxygen extraction rate should be incorporated in the calculations. Considering the physiological pO_2 gradient (arterial $pO_2 \approx 100$ mmHg to venous $pO_2 \approx 40$ mmHg), erythrocytes release only about 20–25% of the bound oxygen (≈4 ml O_2/dl), while pure blood plasma, 5% HSA or conventional saline blood replacement solutions provide approximately 60% of the dissolved oxygen [52]. A different setting arises when ventilating the patient with pure oxygen. Despite the increased pO_2 gradient, the erythrocytes' oxygen release is raised only marginally to a maximum of 25%, whereas the oxygen release of perfluorocarbons is boosted up to about 92% [52]. This means that 64 vol% of the capsules release approximately twice the amount of whole blood (15 g/dl) and even a little more (factor 1.38) than an EC, while 32 vol% capsules release 1.3× more than whole blood (15 g/dl) and nearly equal an EC (factor 0.95, Table 3). Thus, both preparations (32 and 64 vol%) provide theoretically enough oxygen to ensure sufficient oxygenation of a human organism even after a complete exchange transfusion. When compared to the two relevant competitive artificial oxygen carriers based on perfluorocarbons Perftoran® (a 20% perfluorocarbon-based emulsion approved for human use in Russia, Kazakhstan, Kirgizstan, Mexico and Ukraine [11,12]) and Oxygent® (a non-approved 60% perfluorocarbon-based emulsion), the oxygen transport capacity and the oxygen release of the capsules (32 and 64 vol%) can be ranked between the two products (Fig. 4B).

3.5. Compatibility after intravenous administration

To point it out right away, all animals tolerated the intravenous administration of the capsules (32 and 64 vol%, corresponding to 1.7 g/kg KGW and 3.3 g/kg KGW perfluorodecalin, respectively) without difficulty. With a maximum of only 3.3 g perfluorodecalin/kg KGW toxic effects of perfluorodecalin *per se* were not to be expected, as the absolute harmless doses of perfluorocarbons after intravenous administration range from 2.7 to 9 g perfluorocarbon/kg (depending the perfluorocarbon and on the species, 2.7 g in rabbits, 9 g in monkeys) [55]. In trials with Fluosol®, patients received up to 5 g perfluorocarbon/kg [55].

Furthermore the applied dose of 20 ml/kg KGW × h of capsules or control solution corresponds to 1/6 of the blood volume of the rat. This volume equals the volume of 3 red blood cell concentrates when calculated for a human adult (5 l blood, 1/6 = 833 ml).

Despite good general compatibility, some dose-dependent effects could be observed after administration of capsules revealing slight disturbances in acid-base metabolism and minor cellular damage when compared to animals receiving 5% HSA without capsules. The mean hematocrit of all animals was about 40% (5% HSA: 42.12%, 32 vol%: 39.93% and 64 vol%: 39.02%). While pH and pCO_2 were nearly unaffected (Fig. 5A–C), application of capsules (32 and 64 vol%) tended to result in a higher pO_2 compared to treatment with 5% HSA only (Fig. 5E). This shows, that, as expected, capsules contribute to increase the partial pressure. Plasma lactate concentration doubled (32 vol%) or rather increased 1.5-fold (64 vol%) during the post-infusion period (Fig. 5D). A correlating trend was observed for the base excess decreasing up to −4.6 mmol/l 120 min post-infusion of 32 vol% capsules before recovering into the physiological interval 180 min post-infusion. In contrast, base excess after infusion of 5% HSA or 64 vol% capsules oscillated within the physiological range during the entire experimental period (Fig. 5B). Obviously, the elevated plasma level of lactate was one reason for the distinct decrease of base excess after infusion of 32 vol% capsules (Fig. 5D). However, the moderate increase in the plasma level of lactate after infusion of 64 vol% capsules 120–150 min post-infusion was not reflected in the base excess (Fig. 5B and D). Hypoxia certainly was not the reason for the increased levels of lactate, as pO2 oscillated around 500 mmHg during the post-infusion period in all animals that had been treated with capsules (Fig. 5E). However, as the concentrations of lactate and glucose correlated inversely (Fig. 5F), excess glycolysis could have caused the increase in lactate. Glycolysis requiring NAD^+ could have forced NAD^+-recycling via lactate dehydrogenase leading to increased concentrations of lactate because the ox-phos shuttles might have been overwhelmed [56]. Increasing plasma activity of cellular enzymes such as LDH and CK indicated (gradual) cellular damage throughout the post-infusion period (Fig. 6C and D). As the microcirculation of the *musculus gastrocnemius* and the creatinine level in plasma as well as kidney tissue architecture turned out to be normal (data not shown and Fig. S3A and B), skeletal muscle or kidney damage seemed unlikely. Hepatic injury also was improbable because only ASAT activity in plasma increased significantly while ALAT activity was hardly affected, especially when only 32 vol% capsules had been administrated (Fig. 6A and B). Furthermore, the liver as origin of LDH and CK could also be excluded, because hepatic microcirculation (Fig. 7B and C) was perfectly intact and no tissue damage could be observed after microscopic investigation of the liver tissue (Fig. S3C and D). Possibly CK and LDH rather originated from damaged spleen tissue that could be verified in histological evaluation (Fig. 8). Stress fibers containing CK [57] are located in the splenic sinus endothelium and support the filtration of blood through

Table 3
Comparison of the oxygen capacities of blood at relevant hemoglobin concentrations and the albumin-derived perfluorocarbon-based capsules with a volume fraction of 64 vol% at a pO_2 of 500 mmHg.

	Whole blood (5 g/dl)	Whole blood (15 g/dl)	EC	Capsules (32 vol%)	Capsules (64 vol%)
Oxygen capacity (ml O_2/dl)	6.7	~20	~27	5.8	8.5
Oxygen release (ml O_2/dl)	1.7	~4	~5.5	5.2	7.6

inter-endothelial gaps into the sinus lumen [58]. The intravascular presence of capsules might have increased shear forces exerting on the endothelium and thus caused damage of splenic stress fibers (releasing CK) and endothelial cells (releasing ASAT and LDH). As the spleen displays the main filter organ with a very active immune defence, it is already described, that nanoparticles deposit here before being eliminated by the immune cells [59,60]. This uptake into RES cells is very typically reflected by transient vacuolization of macrophages after application of different perfluorocarbon-based emulsions [61,62] and also happened after the application of albumin-derived perfluorocarbon-based capsules (Fig. 8). While alterations in tissue architecture such as vacuolized macrophages were observed after capsule administration (Fig. 8B + E), spleen tissue remained intact when only 5% HSA was infused (Fig. 8A + C). Although a nearly identical percentage area of stained macrophages could be detected between the animals receiving 5% HSA or 32 vol% capsules, respectively (Fig. 8F), the vacuolization after capsule treatment stands out clearly. Similar perfluorocarbon-based artificial oxygen carriers with different wall materials showed divergent organ damage. Poly(*n*-butyl-cyanoacrylate) coated capsules primarily damaged kidney and spleen [22], while poly(ethylene glycol)-poly(lactide-*co*-glycolide) coated capsules impaired liver and spleen [19].

As the 32 vol% capsules showed less side-effect than the 64 vol% preparation, all following experiments were restricted to the application of 32 vol% capsules. Up until now it has been thought, that intravenous use of perfluorocarbons commonly is associated with a more or less profound transient systemic hypotension [63–65]. Unfortunately, this side-effect was verified by us when investigating related perfluorocarbon-based capsule systems in the past [19,22]. Both poly(*n*-butyl-cyanoacrylate) coated capsules and poly(ethylene glycol)-poly(lactide-*co*-glycolide) coated capsules did evoke a transient systemic hypotension [19,22]. With albumin as wall material, the systemic circulation (Fig. 7A) was not affected after infusion of 32 vol% capsules and body temperature, heart and breathing rate fluctuated within the physiological range to be expected under isoflurane anesthesia during the experimental period (data not shown) [66]. The peripheral microcirculation was only slightly disturbed. At the end of the infusion period, treatment with 32 vol% capsules significantly decreased the number of perfused vessels, as well as the vessel diameter (Fig. 7B and C). Importantly this was only a transient effect as microcirculation restored during the observation period (Fig. 7B). Additionally, although significant the observed differences were not physiologically relevant, because control animals also show about 3% non-perfused vessels [67]. The unaffected macro- and only marginally altered microcirculation represents a great improvement, as in hospitalized patients this lacking side-effect would result in avoiding a pharmacological treatment with steroids [27,65].

3.6. Biodistribution and circulatory half-life

Generally, perfluorocarbon-based artificial oxygen carriers are eliminated from the intravascular system by the reticuloendothelial system. In the case of the capsules used in the experiments presented in this study, the albumin shell is degraded by the proteasome releasing small amounts of perfluorodecalin. The perfluorodecalin diffuses over the cell membrane, binds to lipoproteins and is transported to the lung where it is exhaled because of its high vapour pressure [55]. Tracking the distribution of capsules in the body, revealed capsule accumulation solely in the spleen (Fig. 8C). All other organs did not accumulate capsules (Fig. S4). This distribution pattern was in line with the organ damage observed after tissue section evaluation (Fig. 8A and B) and with the fact, that nanoparticles are entrapped by red pulp macrophages of the spleen after intravenous administration to rats [59,60]. A different distribution pattern had been observed for other perfluorocarbon-based capsules (kidney, spleen and small intestine for poly(*n*-butyl-cyanoacrylate) [22], liver and spleen for poly(ethylene glycol)-poly(lactide-*co*-glycolide)) [19], the wall material seems to influence capsule distribution inside the body. The impact of surface characteristics on biodistribution has been also confirmed by others [59].

To work efficiently as artificial oxygen carriers, capsules should remain for overly long periods in the intravascular system. The circulatory *in vivo* half-life of capsules was calculated to be 158 min with $r^2 = 0.8531$ (Fig. 9). This is much longer than intravascular availability of related systems we tested in the past. Whereas perfluorodecalin-filled poly(*n*-butyl-cyanoacrylate)-coated capsules displayed the shortest half-life (30 min) [22], poly(ethylene glycol)-poly(lactide-*co*-glycolide)-coated capsules achieved 55 min [20]. The wall material seems to strongly influence circulatory half-life, and especially the biopolymer albumin seems to perfectly prolong bioavailability [68], probably as it has evolved over millions of years as physiological transport molecule of compounds in the blood.

4. Conclusions

In this work, nano-sized albumin-derived perfluorocarbon-based artificial oxygen carriers were successfully synthesized with the ultrasonics method. The biocompatible amphiphilic albumin supersedes the use of any additional (potentially harmful) emulsifier. Subsequent characterization of the capsules in varying dispersion media (H_2O, 0.9% NaCl, 5% HSA) revealed differences. Capsules dispersed in 5% HSA performed best. They showed a constant size distribution and did not influence blood viscosity in the tested concentrations. With respect to their intended use as artificial oxygen carriers, the oxygen capacity of the capsules was measured *in vitro*. To compare these results to relevant competitors under *in vivo* conditions (if ventilating with pure oxygen), based on the measured data, the absolute oxygen capacity of the capsules was calculated for $pO_2 = 500$ mmHg. Calculation was easy to perform, as for perfluorocarbons and 5% HSA the oxygen solubility linearly depends on the pO_2. Under *in vivo* conditions, the capsules performed not as good as whole blood (hemoglobin content of 15 g/dl) but better than the competitor Perftoran®, a perfluorocarbon-based emulsion, already approved as an artificial oxygen carrier for human use in Russia, Ukraine, Mexico, Kyrgyzstan and Kazakhstan [11,12].

However, the important parameter for oxygen supply *in vivo* will be the oxygen extraction rate and not the absolute oxygen capacity (discussed above). If calculating the oxygen extraction rate under *in vivo* conditions ($pO_2 = 500$ mmHg) the capsules not only exceeded Perftoran® but also whole blood.

Furthermore perfluorocarbons (other than hemoglobin-based artificial oxygen carriers) remain functional in the presence of gases such as carbon monoxide, nitric oxide or hydrogen cyanide [14–17].

In vivo evaluation showed minimal but dose-dependent side-effects such as elevation of plasma concentration of cellular enzymes (LDH; ASAT, ALAT, CK), a slight impact on acid base metabolism and moderate tissue damage of the spleen, probably because the red pulp macrophages scavenge the capsules. Importantly, macro- and micro-circulation remained unaffected and the capsules showed a respectable circulatory *in vivo* half-life of 158 min.

So finally, in few words albumin-derived perfluorocarbon-based artificial oxygen carriers display a novel relevant artificial oxygen carrier not only to bridge blood loss but also to therapy decompression sickness and smoke poisonings. First *in vivo* evaluation of

therapeutic relevant amounts of capsules with a focus on toxicity showed good biocompatibility. Therefore, albumin-derived perfluorocarbon-based artificial oxygen carriers should be advanced consequentially to functional *in vivo* testing to study their performance on the oxygen supply of an isolated organ or, later, an entire organism without the presence of erythrocytes.

5. Limitations of the study

We assume that the structural composition of the capsule shell is independent of the capsule's diameter. Therefore, in our view, larger capsules produced for LSM and SEM measurements give a good idea of the smaller capsules we used for animal experiments.

Acknowledgement

Scanning electron microscopy (SEM) experiments were performed at the Imaging Center Essen, University Hospital Essen. Especially the help of Prof. Dr. Elke Winterhager and Miss Sylvia Voortmann is gratefully acknowledged.

This research did not receive any specific grant from funding agencies in the public, commercial or not-for-profit sector.

Appendix A. Supplementary material

Supplementary data associated with this article can be found, in the online version, at http://dx.doi.org/10.1016/j.ejpb.2017.02.015.

References

[1] J.L. Carson, P.A. Carless, P.C. Hebert, Transfusion thresholds and other strategies for guiding allogeneic red blood cell transfusion, Cochrane Database Syst. Rev. 4 (2012) CD002042.
[2] G.M. Liumbruno, S. Vaglio, G. Grazzini, D.R. Spahn, G. Biancofiore, Patient blood management: a fresh look at a new approach to blood transfusion, Minerva Anestesiol. (2014).
[3] J.M. Rohde, D.E. Dimcheff, N. Blumberg, S. Saint, K.M. Langa, L. Kuhn, A. Hickner, M.A. Rogers, Health care-associated infection after red blood cell transfusion: a systematic review and meta-analysis, JAMA 311 (2014) 1317–1326.
[4] T. Henkel-Hanke, M. Oleck, Artificial oxygen carriers: a current review, AANA J. 75 (2007) 205–211.
[5] J. Simoni, New approaches in commercial development of artificial oxygen carriers, Artif. Organs 38 (2014) 621–624.
[6] L.M. Williamson, D.V. Devine, Challenges in the management of the blood supply, Lancet 381 (2013) 1866–1875.
[7] Y. Bian, G. Wei, T.M. Chang, Lowering of elevated tissue PCO2 in a hemorrhagic shock rat model after reinfusion of a novel nanobiotechnological polyhemoglobin-superoxide dismutase-catalase-carbonic anhydrase that is an oxygen and a carbon dioxide carrier with enhanced antioxidant properties, Artif. Cells Nanomed. Biotechnol. 41 (2013) 60–68.
[8] C.J. Lewis, J.D. Ross, Hemoglobin-based oxygen carriers: an update on their continued potential for military application, J. Trauma Acute Care Surg. 77 (2014) S216–S221.
[9] Z. Tao, P.P. Ghoroghchian, Microparticle, nanoparticle, and stem cell-based oxygen carriers as advanced blood substitutes, Trends Biotechnol. 32 (2014) 466–473.
[10] D. Wang, J. Sun, S.B. Solomon, H.G. Klein, C. Natanson, Transfusion of older stored blood and risk of death: a meta-analysis, Transfusion 52 (2012) 1184–1195.
[11] C.I. Castro, J.C. Briceno, Perfluorocarbon-based oxygen carriers: review of products and trials, Artif. Organs 34 (2010) 622–634.
[12] P.E. Keipert, Oxygen therapeutics ("blood substitutes") where are they, and what can we expect?, Adv Exp. Med. Biol. 540 (2003) 207–213.
[13] D. Ortiz, M. Barros, S. Yan, P. Cabrales, Resuscitation from hemorrhagic shock using polymerized hemoglobin compared to blood, Am. J. Emerg. Med. 32 (2014) 248–255.
[14] T. Randsoe, O. Hyldegaard, Effect of oxygen breathing and perfluorocarbon emulsion treatment on air bubbles in adipose tissue during decompression sickness, J. Appl. Physiol. 107 (2009) (1985) 1857–1863.
[15] B.D. Spiess, Perfluorocarbon emulsions as a promising technology: a review of tissue and vascular gas dynamics, J. Appl. Physiol. 106 (2009) 1444–1452.
[16] K. Yokoyama, Effect of perfluorochemical (PFC) emulsion on acute carbon monoxide poisoning in rats, Jpn. J. Surg. 8 (1978) 342–352.
[17] H.A. Sloviter, M. Petkovic, S. Ogoshi, H. Yamada, Dispersed fluorochemicals as substitutes for erythrocytes in intact animals, J. Appl. Physiol. 27 (1969) 666–668.
[18] M.C. Clark, D.S. Weiman, J.W. Pate, S. Gir, Perfluorocarbons: future clinical possibilities, J. Invest. Surg. 10 (1997) 357–365.
[19] K.B. Ferenz, I.N. Waack, J. Laudien, C. Mayer, M. Broecker-Preuss, H. de Groot, M. Kirsch, Safety of poly (ethylene glycol)-coated perfluorodecalin-filled poly (lactide-co-glycolide) microcapsules following intravenous administration of high amounts in rats, Results Pharma Sci. 4 (2014) 8–18.
[20] K.B. Ferenz, I.N. Waack, C. Mayer, H. de Groot, M. Kirsch, Long-circulating poly(ethylene glycol)-coated poly(lactid-co-glycolid) microcapsules as potential carriers for intravenously administered drugs, J. Microencapsul. (2013).
[21] M. Kirsch, T. Bramey, I.N. Waack, F. Petrat, C. Mayer, H. de Groot, The necessity for the coating of perfluorodecalin-filled poly(lactide-co-glycolide) microcapsules in the presence of physiological cholate concentrations: Tetronic-908 as an exemplary polymeric surfactant, J. Microencapsul. 29 (2012) 30–38.
[22] J. Laudien, C. Groß-Heitfeld, C. Mayer, H. De Groot, M. Kirsch, K.B. Ferenz, Perfluorodecalin-filled poly(n-butyl-cyanoacrylate) nanocapsules as potential artificial oxygen carriers: preclinical safety and biocompatibility, J. Nanosci. Nanotechnol. 15 (2014) 1–12.
[23] C. Stephan, C. Schlawne, S. Grass, I.N. Waack, K.B. Ferenz, M. Bachmann, S. Barnert, R. Schubert, M. Bastmeyer, H. de Groot, C. Mayer, Artificial oxygen carriers based on perfluorodecalin-filled poly(n-butyl-cyanoacrylate) nanocapsules, J. Microencapsul. 31 (2014) 284–292.
[24] D.A. Ingram, M.B. Forman, J.J. Murray, Activation of complement by fluosol attributable to the pluronic detergent micelle structure, J. Cardiovasc. Pharmacol. 22 (1993) 456–461.
[25] I.N. Kuznetsova, Perfluorocarbon emulsions: stability in vitro and in vivo. A review, Pharm. Chem. J. 37 (2003) 20–25.
[26] R.F. Mattrey, P.L. Hilpert, C.D. Long, D.M. Long, R.M. Mitten, T. Peterson, Hemodynamic effects of intravenous lecithin-based perfluorocarbon emulsions in dogs, Crit. Care Med. 17 (1989) 652–656.
[27] G.M. Vercellotti, D.E. Hammerschmid, P.R. Craddock, H.S. Jacob, Activation of plasma complement by perfluorocarbon artificial blood: probable mechanism of adverse pulmonary reactions in treated patients and rationale for corticosteroids prophylaxis, Blood Transfus 59 (1982) 1299–1304.
[28] G.V. Patil, Biopolymer albumin for diagnosis and in drug delivery, Drug Develop. Res. 58 (2003) 219–247.
[29] L.C. Clark Jr., S. Kaplan, F. Becattini, G. Benzing 3rd, Perfusion of whole animals with perfluorinated liquid emulsions using the Clark bubble-defoam heart-lung machine, Fed. Proc. 29 (1970) 1764–1770.
[30] R. Haruki, T. Kimura, H. Iwasaki, K. Yamada, I. Kamiyama, M. Kohno, K. Taguchi, S. Nagao, T. Maruyama, M. Otagiri, T. Komatsu, Safety evaluation of hemoglobin-albumin cluster "hemoact" as a red blood cell substitute, Sci. Rep. 5 (2015) 12778.
[31] E. Tsuchida, K. Sou, A. Nakagawa, H. Sakai, T. Komatsu, K. Kobayashi, Artificial oxygen carriers, hemoglobin vesicles and albumin-hemes, based on bioconjugate chemistry, Bioconjug. Chem. 20 (2009) 1419–1440.
[32] Y. Xiong, Z.Z. Liu, R. Georgieva, K. Smuda, A. Steffen, M. Sendeski, A. Voigt, A. Patzak, H. Baumler, Nonvasoconstrictive hemoglobin particles as oxygen carriers, ACS Nano 7 (2013) 7454–7461.
[33] H.A. Sloviter, T. Kamimoto, Erythrocyte substitute for perfusion of brain, Nature 216 (1967) 458–460.
[34] H.A. Sloviter, H. Yamada, S. Ogoshi, Some effects of intravenously administered dispersed fluorochemicals in animals, Fed. Proc. 29 (1970) 1755–1757.
[35] J.G. Riess, Oxygen carriers ("blood substitutes") – raison d'etre, chemistry, and some physiology, Chem. Rev. 101 (2001) 2797–2920.
[36] D.R. Spahn, K.F. Waschke, T. Standl, J. Motsch, L. Van Huynegem, M. Welte, H. Gombotz, P. Coriat, L. Verkh, S. Faithfull, P. Keipert, G. European, Perflubron Emulsion in Non-Cardiac Surgery Study, Use of perflubron emulsion to decrease allogeneic blood transfusion in high-blood-loss non-cardiac surgery: results of a European phase 3 study, Anesthesiology 97 (2002) 1338–1349.
[37] Z.L. Brookes, S. Kaufman, Effects of atrial natriuretic peptide on the extrasplenic microvasculature and lymphatics in the rat in vivo, J. Physiol. 565 (2005) 269–277.
[38] C. Finder, M. Wohlgemuth, C. Mayer, Analysis of particle size distribution by particle tracking, Part. Part. Syst. Charact. 21 (2004) 372–378.
[39] C.o. Europe, European Pharmacopoeia, 7.0 ed., European Directorate for the Quality of Medicines & Healthcare, 2011.
[40] E.P.a.E. Council, European Commission (2010) Directive 2010/63/EU on Protection of Animals Used for Scientific Purposes, Institute for Health and Consumer Protection, Ispra, Italy, 2010.
[41] L. Brencher, R. Verhaegh, M. Kirsch, Attenuation of intestinal ischemia-reperfusion-injury by beta-alanine: a potentially glycine-receptor mediated effect, J. Surg. Res. 211 (2017) 233–241.
[42] A.G. Webb, M. Wong, K.J. Kolbeck, R. Magin, K.S. Suslick, Sonochemically produced fluorocarbon microspheres: a new class of magnetic resonance imaging agent, J. Magn. Reson. Imaging 6 (1996) 675–683.
[43] C.A. Fraker, A.J. Mendez, L. Inverardi, C. Ricordi, C.L. Stabler, Optimization of perfluoro nano-scale emulsions: the importance of particle size for enhanced oxygen transfer in biomedical applications, Colloids Surf. B: Biointerfaces 98 (2012) 26–35.

[44] V. Centis, C.J. Doillon, P. Vermette, Perfluorocarbon emulsions cytotoxic effects on human fibroblasts and effect of aging on particle size distribution, Artif. Organs 31 (2007) 649–653.
[45] D. Lochmann, J. Weyermann, C. Georgens, R. Prassl, A. Zimmer, Albumin-protamine-oligonucleotide nanoparticles as a new antisense delivery system. Part 1: physiocochemical characterization, Eur. J. Pharm. Biopharm. 59 (2005) 419–429.
[46] J.N. Patton, A.F. Palmer, Physical properties of hemoglobin-poly(acrylamide) hydrogel-based oxygen carriers: effect of reaction pH, Langmuir 22 (2006) 2212–2221.
[47] M. Roser, D. Fischer, T. Kissel, Surface-modified biodegradable albumin nano- and microspheres. II: effect of surface charges on in vitro phagocytosis and biodistribution in rats, Eur. J. Pharm. Biopharm. 46 (1998) 255–263.
[48] J. Gong, M. Huo, J. Zhou, Y. Zhang, X. Peng, D. Yu, H. Zhang, J. Li, Synthesis, characterization, drug-loading capacity and safety of novel octyl modified serum albumin micelles, Int. J. Pharm. 376 (2009) 161–168.
[49] H.C. Kwaan, Role of plasma proteins in whole blood viscosity: a brief clinical review, Clin. Hemorheol. Microcirc. 44 (2010) 167–176.
[50] J.G. Riess, Perfluorocarbon-based oxygen delivery, Artif. Cells Blood Substit. Immobil. Biotechnol. 34 (2006) 567–580.
[51] D.R. Spahn, Blood substitutes. Artificial oxygen carriers: perfluorocarbon emulsions, Crit. Care 3 (1999) R93–R97.
[52] N.S. Faithfull, The concept of hemoglobin equivalency of perfluorochemical emulsion, Adv. Exp. Med. Biol. 530 (2003) 271–285.
[53] R. Weinstein, 2012 Practice Guide on Clinical Transfusion, American Society of Hematology, Washington, 2012.
[54] J.L. Carson, Blood transfusion and risk of infection: new convincing evidence, JAMA 311 (2014) 1293–1294.
[55] S.F. Flaim, Pharmacokinetics and side effects of perfluorocarbon-based blood substitutes, Artif. Cells Blood Substit. Immobil. Biotechnol. 22 (1994) 1043–1054.
[56] B. Phypers, J.M.T. Pierce, Lactate physiology in health and disease, Contin. Educ. Anesth. Crit. Care Pain 6 (2006) 128–132.
[57] B.S. Eckert, S.J. Koons, A.W. Schantz, C.R. Zobel, Association of creatine phosphokinase with the cytoskeleton of cultured mammalian cells, J. Cell Biol. 86 (1980) 1–5.
[58] D. Drenckhan, J. Wagner, Stress fibers in the splenic sinus endothelium in situ: molecular structure, relationship to the extracellular matrix, and contractility, J. Cell Biol. 102 (1986) 1738–1747.
[59] M. Demoy, J.P. Andreux, C. Weingarten, B. Gouritin, V. Guilloux, P. Couvreur, Spleen capture of nanoparticles: influence of animal species and surface characteristics, Pharm. Res. 16 (1999) 37–41.
[60] M. Demoy, S. Gibaud, J.P. Andreux, C. Weingarten, B. Gouritin, P. Couvreur, Splenic trapping of nanoparticles: complementary approaches for in situ studies, Pharm. Res. 14 (1997) 463–468.
[61] S.F. Flaim, D.R. Hazard, J. Hogan, R.M. Peters, Characterization and mechanism of side-effects of Oxygent HT (highly concentrated fluorocarbon emulsion) in swine, Artif. Cells Blood Substit. Immobil. Biotechnol. 22 (1994) 1511–1515.
[62] S. Caiazza, C. Fanizza, M. Ferrari, Fluosol 43 particle localization pattern in target organs of rats, Virchows Arch. [Pathol. Anat.] 404 (1984) 127–137.
[63] K.K. Tremper, A.E. Friedman, E.M. Levine, R. Lapin, D. Camarillo, The preoperative treatment of severely anemic patients with a perfluorochemical oxygen-transport fluid, Fluosol-DA, N. Engl. J. Med. 307 (1982) 277–283.
[64] K. Waxman, C.K. Cheung, G.R. Mason, Hypotensive reaction after infusion of a perfluorochemical emulsion, Crit. Care Med. 12 (1984) 609–610.
[65] N.S. Faithfull, C.E. King, S.M. Cain, Peripheral vascular responses to fluorocarbon administration, Microvasc. Res. 33 (1987) 183–193.
[66] C.-H. Yang, M.Y.-C. Chen, T.-I. Chen, C.-F. Cheng, Dose-dependent effects of isofluraneon cardiovascular function in rats, Tzu Chi Med. J. 26 (2014) 119–122.
[67] T.A. Koeppel, J.C. Thies, P. Schemmer, M. Trauner, M.M. Gebhard, G. Otto, S. Post, Inhibition of nitric oxide synthesis in ischemia/reperfusion of the rat liver is followed by impairment of hepatic microvascular blood flow, J. Hepatol. 27 (1997) 163–169.
[68] F. Kratz, Albumin as a drug carrier: design of prodrugs, drug conjugates and nanoparticles, J. Control. Release 132 (2008) 171–183.